JOURNAL OF CATALYSIS **102**, 316–327 (1986)

Desorptive Diffusion of Benzene in H-ZSM-5 under Catalytic Conditions Using Dynamic Sorption/Desorption Technique

V. R. CHOUDHARY[1] AND K. R. SRINIVASAN

Chemical Engineering Division, National Chemical Laboratory, Pune 411 008, India

Received May 17, 1985; revised July 9, 1986

A dynamic sorption/desorption technique using a gas chromatograph for obtaining precise desorption kinetic data on zeolites in the short initial period of desorption (even in the first few seconds of desorption) at temperatures at which catalytic reactions occur has been described. The application of this method for studying desorptive diffusion of benzene (in presence of helium) in H-ZSM-5 (Si/Al = 22.0) zeolite at the temperatures at which catalytic processes occur has made it possible to estimate the diffusion coefficients from the desorption data using the simple $\sqrt{t}$ – law. This is not possible by any known gravimetric or volumetric method. The diffusion of benzene in the zeolite at 523–673 K is highly concentration dependent; it increases almost exponentially with the initial sorbate loading, even at lower intracrystalline sorbate concentrations. It is also highly temperature dependent; the activation energy for the diffusion was determined to be 64.4 kJ · mol^{-1}.

INTRODUCTION

ZSM-5 type zeolites have shown high promise as potential catalysts in a number of commerical processes, such as conversion of hydrocarbons, production of olefins, aromatics, and gasoline from methanol, and also in syngas conversion to petrochemical feed stock and gasoline (*1*). Intracrystalline diffusion plays (*2*) a very vital role in these highly shape-selective zeolites in deciding the product distribution (or selectivity) in the catalytic processes. The understanding of the diffusion phenomenon in these zeolites is therefore of great importance.

Haag *et al.* (*3*) have determined the diffusivities of straight and branched chain hydrocarbons in ZSM-5 under reaction conditions at 811 K by studying catalytic cracking of C_6–C_9 hydrocarbons on the zeolite crystallites of different sizes. The diffusivity values were estimated from the knowledge of the effectiveness factors, the intrinsic reaction rate constant, and the crystallite size. A few more studies on the diffusion in ZSM-5 type zeolite at lower temperatures have been reported. Heering *et al.* (*4*) and Doelle *et al.* (*5*) measured diffusivities of dimethyl ether (at 293 and 333 K) and benzene (at 293 and 313 K) in H-ZSM-5 from sorption kinetics by gravimetric method in a closed system. Wu *et al.* (*6*) studied diffusion of *n*-hexane, cyclohexane, benzene, and xylenes in silicalite at 293–473 K using gravimetric method. Le Van MaO *et al.* (*7*) have determined diffusivity of xylene isomers in H-ZSM-5 at 333 K by measuring sorption at constant pressure gravimetrically. Recently, Nayak and Riekert (*8*) have studied sorption and diffusion of *n*-hexane, benzene, toluene, and *p*-xylene in pentasil zeolites (viz. H-ZSM-5) at 298 K. The diffusion in pentasil zeolites has been reviewed by Ruthven (*9*).

The diffusion in ZSM-5 zeolite is expected to be highly temperature and concentration dependent. Hence, in order to understand the diffusion/reaction interaction, which decides the product selectivity (*2*), it is highly desirable to investigate the diffusion in the shape selective zeolite under catalytic conditions (in other words, at

---

[1] To whom all the correspondence should be addressed.

0021-9517/86 $3.00

the temperatures at which catalytic processes occur).

Diffusion in zeolite is most commonly studied by measuring sorption/desorption kinetics using gravimetric and volumetric methods. The major limitation of these experimental methods is that it is not possible to obtain reliable measurements in the first few seconds (*10*). This limits the applicability of the simple $\sqrt{t}$ − law (*11*) for the system involving rapid sorption/desorption process and it becomes essential to consider the shape and size distribution of the zeolite crystals for obtaining reliable values of diffusion coefficient (*10, 12*). Also, the interparticle mass transfer and heat transfer effects (*13, 14*) are large since the sorbate does not flow through the zeolite particles. Hence, there is a need for developing an experimental method for obtaining sorption/desorption kinetic data, uncontaminated by the heat and mass transfer effects, in the short initial period (<15 sec).

In the present paper, a dynamic sorption/desorption technique for measuring precisely desorption kinetics on zeolites in the short initial period of the desorption under catalytic conditions has been described. Desorptive diffusion of benzene in H-ZSM-5 at 523–673 K and at different initial concentrations of sorbed benzene has been investigated.

EXPERIMENTAL

Materials. High-purity helium (>99.99%) was obtained from Air Products. Benzene (AnalaR, BDH) was further purified by fractional distillation and stored over activated molecular sieves.

H-ZSM-5 zeolite (Si/Al = 22.0 and H^+ − exchange = 99%) was obtained from its NH_4—from by deammoniating it at 773 K for 12 hr in air. The zeolite was pressed without binder and crushed to particles of about 0.2 mm in size. The detailed procedures for the preparation and characterization of the zeolite is given in an earlier reference (*15*).

The size and morphology of the zeolite crystals were determined using a Cambridge Stereoscan Model 150 Scanning electron microscrope. The shape of the crystals was nearly spherical and their average size was 1.46 μm.

The zeolite contained 1.6 strong acid sites per unit cell as measured in terms of the amount of pyridine irreversibly sorbed at 673 K. Detailed information on the acid strength distribution on the zeolite is given in an earlier reference (*16*).

The intracrystalline sorption capacity of the zeolite for *n*-hexane and benzene at 303 K was found to be 0.18 and 0.13 $cm^3 \cdot g^{-1}$, respectively. The intercrystalline (macro) pore volume of the zeolite particle measured by the liquid isooctane penetration method using a specific gravity bottle (*17*) was found to be 0.27 $cm^3 \cdot g^{-1}$. (Liquid isooctane penetrates only the macropores and not the zeolite crystals.)

Experimental arrangement. The experimental setup for measuring kinetics of desorption of benzene from the zeolite in the flow of helium consisted mainly of a Perkin–Elmer Sigma 3B gas chromatograph fitted with a flame ionization detector, a zeolite column, and a benzene vapor saturator.

The zeolite column (made of stainless steel, i.d. = 4 mm, o.d. = 6 mm, and length = 30 mm) was packed with 50 mg of the zeolite particles (0.2 mm size) between quartz wool plugs. The dimensions of the zeolite bed were 4 mm (diam.) × 3 mm (length). One end of the column was connected to the detector through a 10-cm-long stainless-steel capillary tube (i.d. = 0.75 mm and o.d. = 1.5 mm) and the other end through a 50-cm-long stainless-steel capillary, which acted as a preheater.

The saturator consisted of a packed bed of alumina pellets with their pores filled with liquid benzene. When helium (precooled to the temperature of the saturator) was passed through the saturator, an effluent helium saturated with benzene vapor at the temperature of the saturator could be obtained.

To measure the sorption and desorption of benzene, use of two helium streams was made. The first stream was passed directly into the zeolite column, while the second was passed through the precooler, the saturator, and the condenser, all three having been maintained at the same temperature. The two streams, the pure helium stream and the benzene-saturated helium stream, met in the injector. The flow rates of the two streams could be varied as desired and measured with capillary flow meters. The benzene-saturated helium stream could be passed continuously through the zeolite bed or bypass with the help of a three-way valve. The bypass was connected to a pressure head (a glass tube dipped in a column of water whose height could be varied) so that the inlet pressure at the three-way valve could be equalized to the pressure in the injector. With this arrangement, when the second stream was introduced into the injector by turning the three-way valve, a continuous undisturbed stream flow through the bed was assured.

The partial pressure of benzene in the helium stream could be varied by varying the temperature of the saturator (258–293 K) and also by adjusting the flow rates of the two streams.

The detector response was found to be linear with respect to the partial pressure of benzene.

Experimental procedure. The zeolite was pretreated *in situ* by heating it in a flow of helium (50 $cm^3 \cdot min^{-1}$) at 673 K (heating rate = 10 $K \cdot min^{-1}$) for 4 hr. The flow rate of pure helium (first stream) was increased to 200 $cm^3 \cdot min^{-1}$ and the desired zeolite column temperature attained. The second helium stream containing benzene at a known concentration was then introduced in the zeolite column and the saturation of the zeolite at that benzene concentration was continued for 30 min. This duration was found to be more than sufficient for sorption equilibrium to be attained. After the saturation, the helium stream containing benzene was bypassed and the benzene sorbed in the zeolite was allowed to desorb in the flow of pure helium. The initial part of the desorption (during the first 10–15 min) was carried out isothermally and this was followed by the temperature-programmed desorption (TPD) of the sorbate still remaining in the zeolite. The final temperature and the heating rate for the TPD were 673 K and 20 $K \cdot min^{-1}$, respectively. After the final temperature was reached, the desorption was allowed to continue at 673 K until the recorder pen reached the baseline at the maximum sensitivity of the detector. During the initial period of desorption, (3–4 min), the chromatogram was recorded at a very high chart speed (30 $cm \cdot min^{-1}$), which was reduced to 30 $cm \cdot hr^{-1}$ during the rest of the desorption. The detector sensitivity was also increased from time to time to increase the measuring accuracy of the desorption data. The procedure for obtaining sorption/desorption chromatogram is illustrated in Fig. 1.

The amount of benzene sorbed irreversibly in the zeolite and on the walls of the column and the connecting capillary was found to be negligibly small at 523–673 K.

Evaluation of desorption kinetic data. The evaluation of desorption kinetic data from the desorption chromatogram is illustrated in Fig. 1. The values of Q_t/Q_∞ (where Q_t and Q_∞ are the amount of benzene desorbed at time t and ∞, respectively) at different desorption periods (covering the isothermal desorption range) was obtained from the relation

$$Q_t/Q_\infty = A_t/A_\infty \qquad (1)$$

where, A_t is the area (normalized) under the desorption curve from time $t = 0$ to $t = t$; A_∞, the total area (normalized) under the desorption curve. The area under the desorption curve was determined by the cut-and-weigh method.

The amount of the sorbate in the zeolite crystals before the start of desorption $[(q_a)_i]$ was obtained from the total area under the desorption curve,

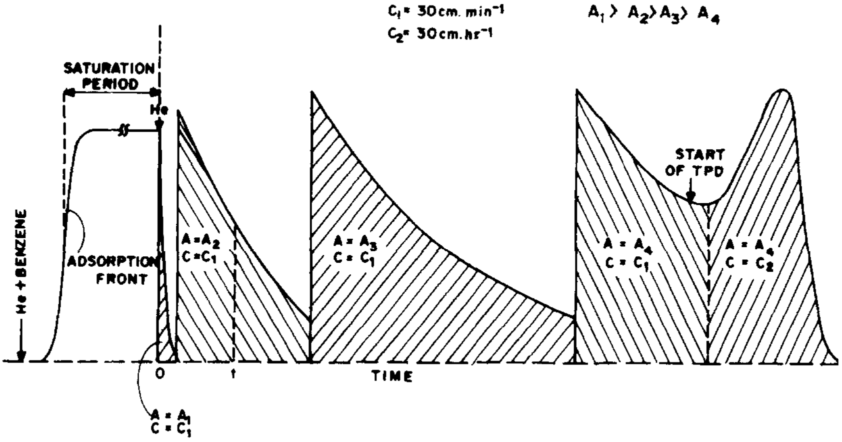

FIG. 1. Evaluation of desorption kinetics from desorption chromatogram. A, attenuation; C, chart speed.

$$(q_a)_i = A_\infty / sm \qquad (2)$$

where, s is the detector response and m is the mass of zeolite. By adjusting the experimental conditions accordingly, the desorption at near zero concentration of the sorbate in the mobile phase could be ensured. This was achieved in the present case by using a very small (50 mg) zeolite sample kept in a shallow bed reactor (diam. = 4.0 mm and length = 3.0 mm) and by keeping the flow rate of helium high (200 cm^3 min^{-1}).

RESULTS AND DISCUSSION

Desorptive Intracrystalline Diffusion

In the overall sorption process in the zeolite particles, the following mass transfer processes are involved: (1) external (film diffusional) mass transfer from bulk gas phase to the external surface of the zeolite particles through the gas film surrounding them; (ii) diffusion in macro (intercrystalline) pores of the zeolite particles; (iii) diffusion and sorption in micro (intracrystalline) pores of the zeolite particles.

In the case of desorption, the above steps occur in the reverse order. Since one or more of the above processes may control the rate of sorption/desorption under a particular set of experimental conditions, it is essential to ensure that the sorption/desorption is controlled only by the intracrystalline mass transfer for obtaining intracrystalline diffusivity from sorption/desorption kinetics. To achieve this, the effect of gas flow rate and particle size of the zeolite on the desorption kinetics was studied. Figure 2 shows that changing the flow rate of helium from 100 to 200 $cm^3 \cdot min^{-1}$, and the zeolite particle size from 0.2 to 0.1 mm did not result in any significant change in the desorption kinetics at 673 K, the maximum temperature. This indicates that the desorption is not controlled either by the external mass transfer or by the intercrystalline (macropore) mass transfer. Since the diffusion of benzene (kinetic molecular diam. = 0.585 nm) in H-ZSM-5 (channel diam. = 0.52–0.56 nm) is expected to be activated, the desorption kinetic data obtained at the lower temperatures (less than 673 K) are expected to fall in the intracrysalline diffusion control regime only.

The Q_t/Q_∞ (fraction desorbed) vs $t^{1/2}$ curves for the desorption of benzene from the zeolite at different intracrystalline concentrations of benzene at 523, 573, 623, and 673 K are presented in Figs. 3, 4, 5, and 6, respectively. The benzene sorption isotherms are given in Fig. 7.

The values of desorption diffusion coefficient for benzene in the zeolite have been obtained from the slopes of the initial linear portion of Q_t/Q_∞ vs $t^{1/2}$ curves using the simple $\sqrt{t}$ − law (*11*):

$$Q_t/Q_\infty = 6[D/(\pi r^2)]^{1/2} \cdot t^{1/2} \quad (3)$$

where, D is the desorptive diffusion coefficient; and r, the radius of zeolite crystal. The values of D at the different initial intracrystalline sorbate loadings are given in Table 1. The concentration dependence of the diffusion in the zeolite is shown in Fig. 8.

The results reveal a very strong dependence of the diffusivity of benzene on the initial intracrystalline sorbate concentration. Even at very low sorbate loadings, there is a very marked increase in the diffusion coefficient with the increase in the sorbate loading.

The data in Table 1 also reveal a strong influence of temperature on the diffusion. The temperature dependence of the diffusion coefficient corresponding to the same $(q_a)_i$ value (10.0 μmol · g^{-1}) according to the Arrhenius-type expression

$$D = A\exp(-E/RT) \quad (4)$$

is shown in Fig. 9. The plot of ln D vs $1/T$ is linear. The values of activation energy (E) and preexponential factor (A) were estimated to be 64.4 kJ · mol^{-1} and 14.3×10^{-6} cm^2 · sec^{-1}, respectively. These results indicate that the diffusion of benzene in H-ZSM-5 is a highly activated one.

The concentration dependence of diffusivity is frequently expressed by the relation (*18*)

$$D = D_0(\partial \ln p/\partial \ln q) \quad (5)$$

where, D_0 is the corrected (or limiting) diffusivity. The values of D_0 for the present system are included in Table 1. The results indicate that D_0, also, shows concentration dependence; it increases with the intracrystalline concentration. The effect of concentration on D_0 is, particularly, very significantly at higher temperatures. A very strong concentration dependence of cor-

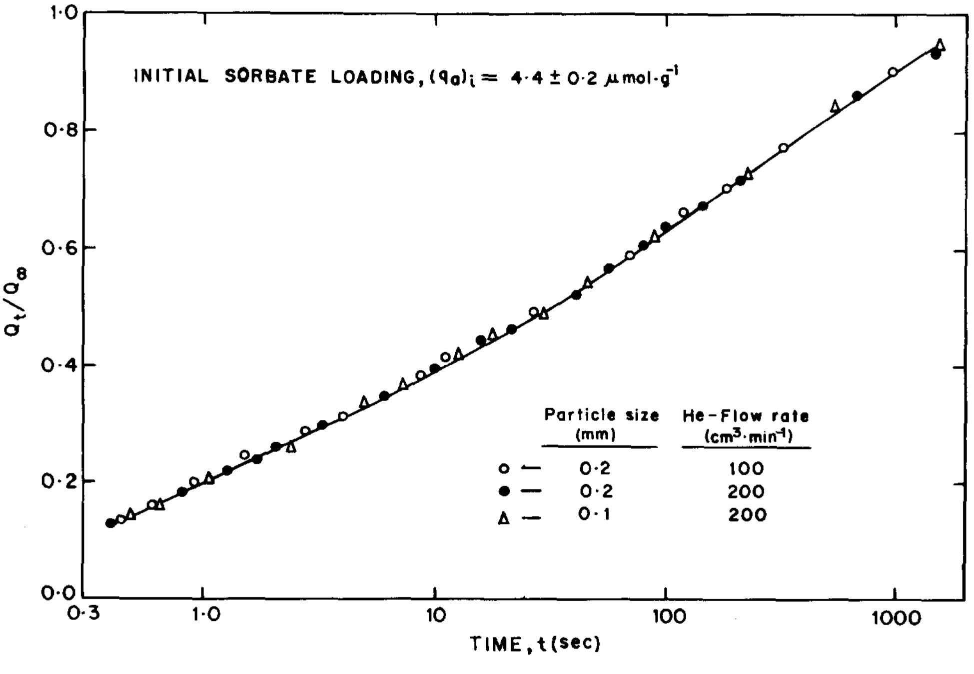

FIG. 2. Kinetics plots (Q_t/Q_∞ vs t) for the desorption of benzene at 673 K from H-ZSM-5 of different particle sizes and at different flow rates.

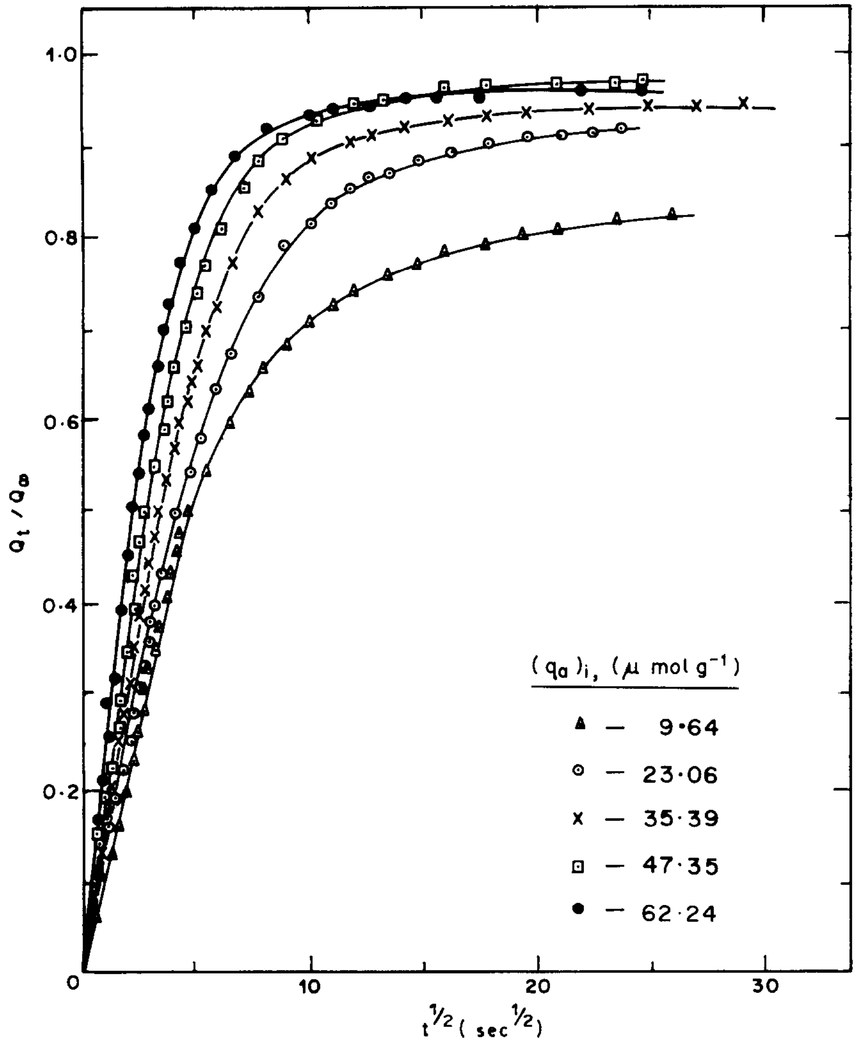

FIG. 3. Q_t/Q_∞ vs $t^{1/2}$ plots for the desorption of benzene from H-ZSM-5 at 523 K.

rected diffusivity for sorption of hydrocarbons in 13X zeolite has also been observed earlier (*18*). Corrected diffusivity need not necessarily be concentration independent, particularly, at higher concentration level outside Henry's law (*9*, *18*).

In the earlier low temperature gravimetric sorption studies, the diffusivity of benzene in ZSM-5 zeolites was obtained as follows: in H-ZSM-5 at 303 K, 2.4×10^{-10} cm^2 · sec^{-1} (*4*, *5*); in H-ZSM-5 at 298 K, $\simeq 6 \times 10^{-12}$ cm^2 · sec^{-1} (*8*); in ZSM-5 at 303 K, 8.6×10^{-12} cm^2 · sec^{-1} (*19*); in Na-ZSM-5 at 303 K, 7.0×10^{-12} cm^2 · sec^{-1} (*20*); and in silicalite at 293 K, 8.6×10^{-12} cm^2 · sec^{-1} (*6*).

The present study shows that the diffusion of benzene in H-ZSM-5 zeolite is highly concentration and temperature dependent. Our recent studies (*21*) indicated a strong influence of Si/Al ratio, degree of H$^+$-exchange and pretreatment conditions on the diffusion of benzene in H · Na-ZSM-5. Further, the sorption diffusivity may differ from the desorption diffusivity for ZSM-5 zeolite. Hence, a direct comparison of the above results of benzene sorption diffusion, obtained at lower temperatures, with the present results can not be made.

In the present case, since benzene does not undergo reaction on H-ZSM-5 even at higher temperatures, its desorptive diffusion in the zeolite could be studied under catalytic conditions.

Intracrystalline diffusion coefficients for sorption and desorption of *n*-butane in NaX have been found to be independent of the direction of flux (*14*). However, in case of shape selective zeolite like the one used in the present investigation, the diffusion coefficients obtained from sorption and desorption are expected to be dependent on the direction of the flux because of the following reason.

In the case of sorption, the overall intracrystalline mass transfer in H-ZSM-5 zeolite whose channel diameter (about 0.55 nm) is somewhat smaller than the critical diameter of the diffusing species is expected to be controlled by either of the following of the two processes occurring in series or by a combination of both:

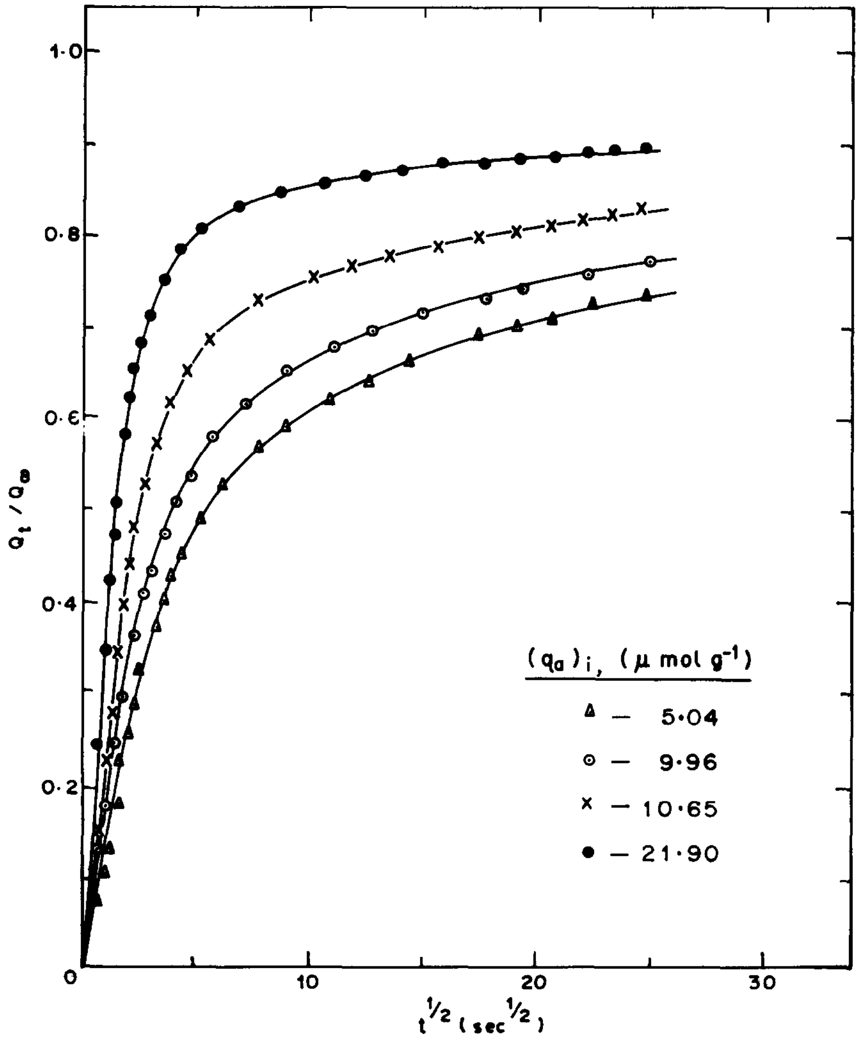

FIG. 4. Q_t/Q_∞ vs $t^{1/2}$ plots for the desorption of benzene from H-ZSM-5 at 573 K.

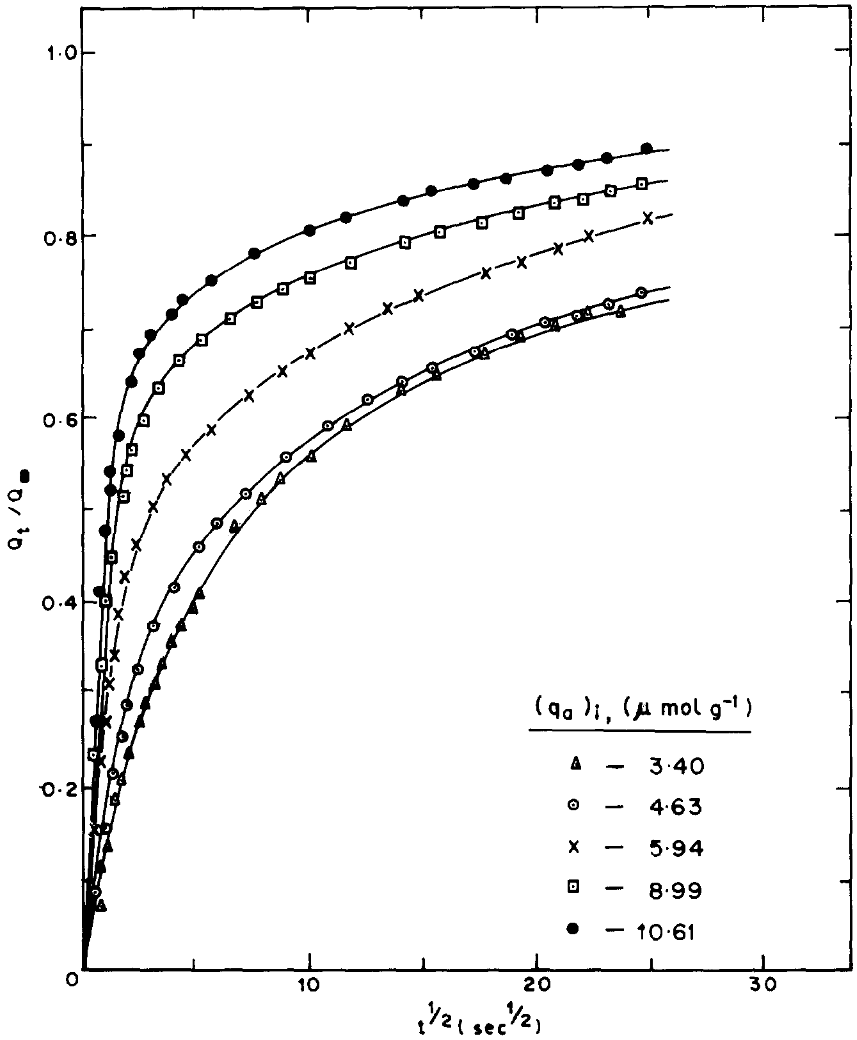

FIG. 5. Q_t/Q_∞ vs $t^{1/2}$ plots for the desorption of benzene from H-ZSM-5 at 623 K.

(i) entrance of diffusing species into the zeolite channels;

(ii) diffusion of the species inside the channels.

The first process becomes very important when the critical diameter of the diffusing species is very close to the channel diameter and the diameters in its other orientations are so large that the entry of the molecule into the channel cannot occur. Here, critical diameter is defined as the diameter of the smallest cylinder that can circumscribe the molecule in its equilibrium conformation that is most favorable for diffusion to occur. The probability of the molecule colliding with the channel opening in its most favorable conformation will vary depending on the configuration of the diffusing species. In the case of benzene, the critical diameter is 0.66 nm and the maximum diameter is 0.74 nm. The diffusion is expected to occur only when a benzene molecule with a conformation having a diameter of 0.66 nm collides with a channel opening. Further, since the benzene molecule is planar, its orientation at the elliptical straight channels (0.51–0.55 nm) should be such that the molecule in its most favorable conformation, aligns itself with the longer axis of the elliptical opening. For all other collisions that do not conform to these requirements, either the entry of the diffusing species into the channel is not permitted or the probability for the entry is very low. It should, however, be noted that this resistance to intracrystalline mass transfer exists only for sorption and not for desorption because, in the desorption, the diffusing species (which are already in their most favorable conformation in the channels) are coming out through the channel openings.

In H-ZSM-5 zeolite, the critical dimension at channel intersections is estimated *(22)* to be 0.9 nm. Since the diameter at the channel intersections is much larger than the channel diameter, the diffusivity at these intersections is expected to be different from that in the channels. The diffusivity in two different channels (ellipitcal straight channels and near circular zigzag channels) is also expected to be different from each other. Also, the diffusing molecule can undergo reorientation at the channel intersections as the molecules can rotate freely in the larger space available. The diffusion of species inside the zeolite channels is, therefore, expected to be independents of the direction of flux. However, the restriction for the entrance of the diffusion species in the channels, which is pertaining to sorption but not desorption, may give rise different values for diffusion coefficients from sorption and desorption experiments. Thus the diffusion in H-ZSM-5 is a complex phenomenon and is also strongly dependent on temperature and concentra-

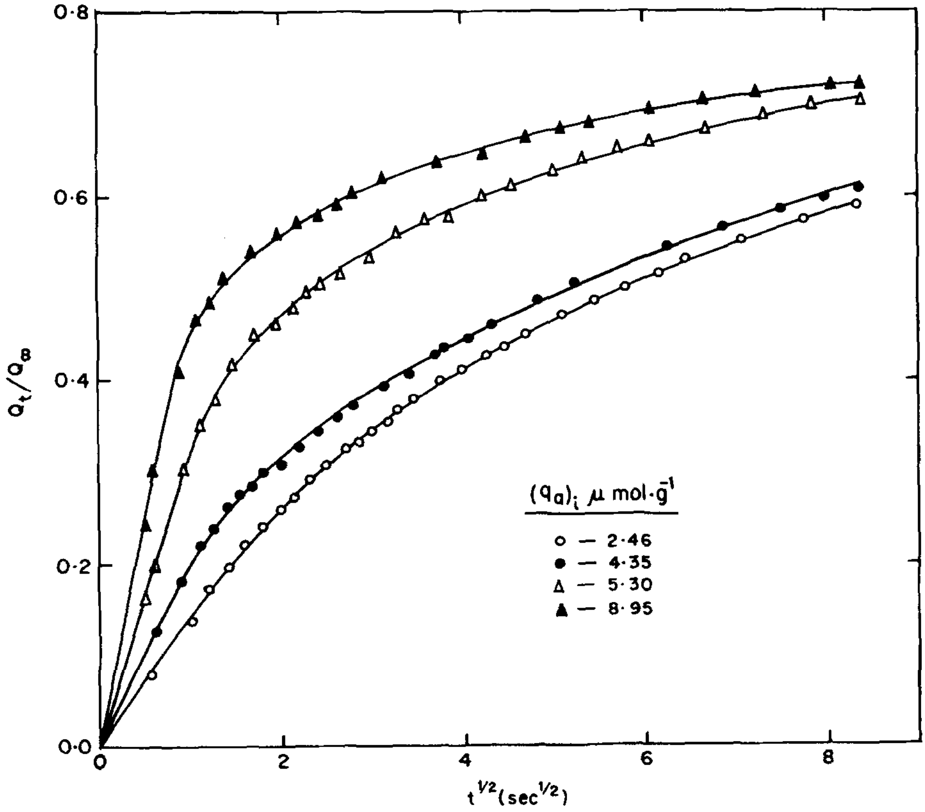

FIG. 6. Q_t/Q_∞ vs $t^{1/2}$ plots for the desorption of benzene from H-ZSM-5 at 673 K.

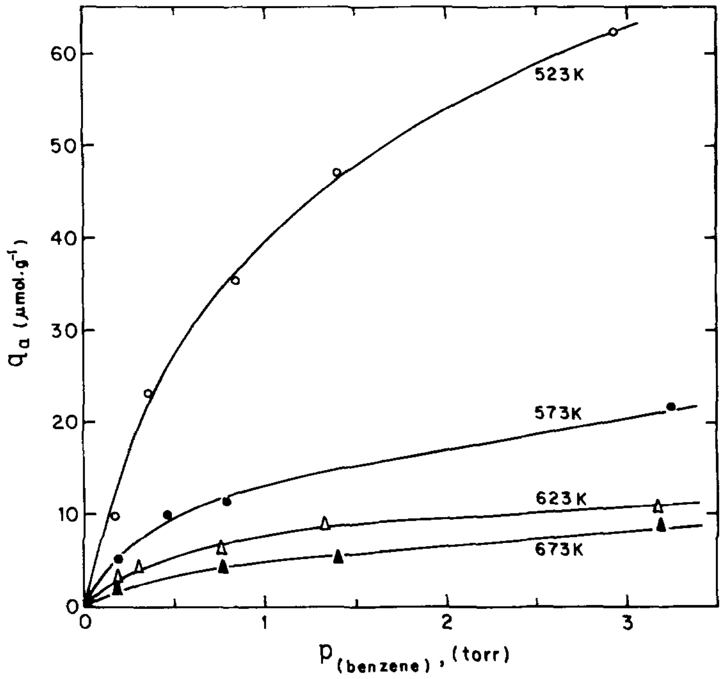

FIG. 7. Isotherms of sorption of benzene in H-ZSM-5 at different temperatures.

TABLE 1

Desorption Diffusion Coefficients for Benzene in the H-ZSM-5 at Different Concentrations of Sorbed Benzene and Temperatures

Temperature (K)	Initial sorbate loading $(q_a)_i$ (μmol · g^{-1})	$(D/r^2) \times 10^3$ (sec^{-1})	$D \times 10^{11}$ (cm^2 · sec^{-1})	$D_0 \times 10^{11}$ (cm^2 · sec^{-1})
523	9.6	1.2	0.6	0.6
	23.1	1.4	0.7	0.6
	35.4	2.2	1.2	0.7
	47.4	2.8	1.5	0.7
	62.3	4.5	2.4	0.8
573	5.0	1.4	0.8	0.5
	10.0	2.6	1.4	0.9
	10.7	5.2	2.7	1.2
	21.9	12.0	6.3	1.9
623	3.4	1.3	0.7	0.4
	4.6	2.0	1.1	0.6
	5.9	5.5	1.3	0.8
	9.0	11.8	6.3	2.0
	10.6	16.2	8.6	2.5
673	2.5	1.7	0.9	0.4
	4.4	3.7	2.0	0.8
	5.3	10.0	5.3	2.2
	9.0	21.8	11.6	4.7

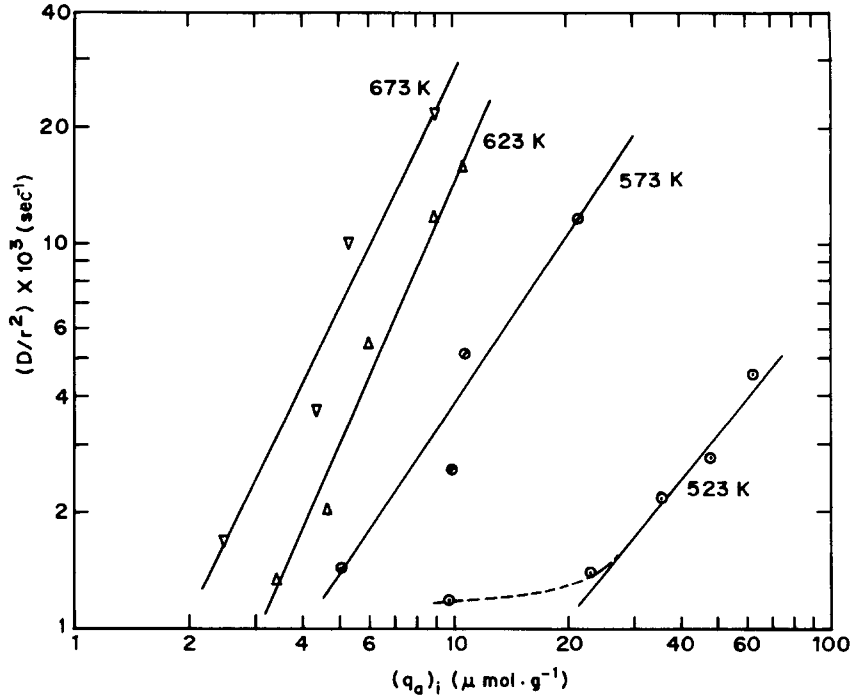

FIG. 8. Concentration dependence of desorptive diffusion of benzene in H-ZSM-5.

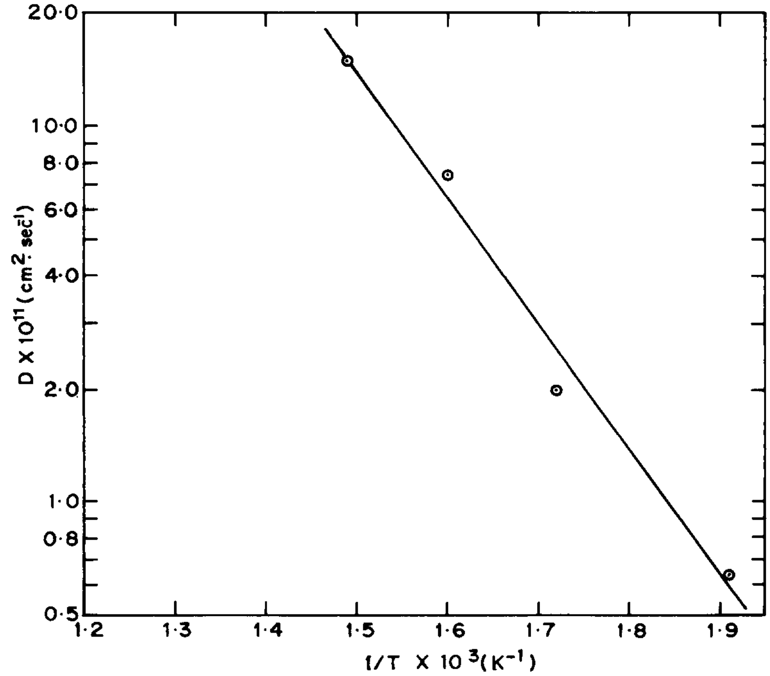

FIG. 9. Temperature dependence of the desorption diffusion coefficient of benzene in H-ZSM-5.

tion even at lower intracrystalline concentrations. For a deeper understanding of the diffusion phenomenon in ZSM-5 type zeolites further extensive work is necessary.

Present Method

The dynamic sorption/desorption method used in the present study has a number of advantages over the conventional volumetric and gravimetric methods for measuring intracrystalline diffusion coefficient. It is possible to obtain precise desorption kinetic data in the first few seconds of the desorption (which is not possible by any other known volumetric or gravimetric method) so that the simplified $\sqrt{t}$ – law could be used for evaluating the diffusion coefficient and it is not necessary to consider the shape and size distribution of the zeolite crystals (*10*). Also, because of the fact that the sorbate is desorbed in the carrier gas flowing through the zeolite particles packed in the column at a high flow rate, the effects of heat transfer which was found to be the rate limiting step in the final approach to equilibrium in the gravimetric and volumetric sorption measurements (*13, 14, 23–26*) and interparticle mass transfer which is very significant in case of the gravimetric sorption/desorption measurements (*13, 14*) on the desorption kinetics are eliminated. The zeolite column is kept in a well-mixed air oven of the gas chromatograph; hence, the sorption/desorption is expected to occur under isothermal conditions.

CONCLUSIONS

Desorption diffusion in zeolites under catalytic conditions can be conveniently studied by the present dynamic sorption/desorption technique using a gas chromatograph. This technique allows the desorption measurements to be carried out in a very short initial period of desorption and, therefore, it is possible to use the simple $\sqrt{t}$ – law for estimating the diffusion coefficients.

The desorption diffusion of benzene in the H-ZSM-5 zeolite at 523–673 K is highly concentration dependent; it increases with the intracrystalline concentration. The corrected diffusivity also shows a strong concentration dependence. The diffusion is a highly activated process.

REFERENCES

1. Scott, J., Ed., "Zeolite Technology and Applications: Recent Advances." Noyes Data Corp., New Jersey, 1980.
2. Weisz, P. B., *Pure Appl. Chem.* **52,** 2091 (1980).
3. Haag, W. O., Lago, R. M., and Weisz, P. B., *Discuss. Faraday Soc.* **72,** 317 (1981).
4. Heering, J., Kotter, M., and Reikert, L., *Chem. Eng. Sci.* **37,** 581 (1982).
5. Doelle, H. J., Heering, J., Riekert, L., and Marosi, L., *J. Catal.* **71,** 27 (1981).
6. Wu, P., Debebe, A., and Ma, Y. H., *Zeolites* **3,** 118 (1983).
7. Le Van MaO, R., Ragaini, V., Leofanti, G., and Fois, R., *J. Catal.* **81,** 418 (1983).
8. Nayak, V. S., and Riekert, L., Int. Symp. Zeolite Catalysis, May 13–16, 1985, Siofok (Hangery), p. 157 (preprints of papers).
9. Ruthven, D. M., *AIChE Symp. Ser.* **80,** 21 (1984).
10. Loughlin, K. F., Derrah, R. I., and Ruthven, D. M., *Canad. J. Chem. Eng.* **49,** 66 (1971).
11. Barrer, R. M., *Adv. Chem. Ser.* **102,** 21 (1971).
12. Ruthven, D. M., and Loughlin, K. F., *AIChE Symp. Ser.* **67,** 35 (1971).
13. Doelle, H. J., and Riekert, L., *Angew. Chem. Int. Ed. Engl.* **18,** 266 (1979).
14. Doelle, H. J., and Riekert, L., *ACS Symp. Ser.* **40,** 401 (1977).
15. Nayak, V. S., and Choudhary, V. R., *Appl. Catal.* **4,** 333 (1982).
16. Choudhary, V. R., and Nayak, V. S., *Mater. Chem. Phys.* **11,** 515 (1984).
17. Choudhary, V. R., and Singh, A. P., *Zeolites* **6,** 206 (1986).
18. Ruthven, D. M., *ACS Symp. Ser.* **40,** 320 (1977).
19. Wu, P., Debebe, A., and Ma, Y. H., AIChE Winter Meeting, Orlando, Fla., paper 55a (1982).
20. Wu, P., and Ma, Y. H., *in* "Proc. 6th Int. Zeolite Conf., Reno," July 10–15, 1983 (D. Olson and A. Bisio, Eds.), p. 251. Butterworths, London, 1984.
21. Choudhary, V. R., and Srinivasan, K. R., *J. Catal.* **102,** 328 (1986).
22. Derouane, E. G., and Gabelica, Z., *J. Catal.* **65,** 486 (1980).
23. Kondis, E. F., and Dranoff, J. S., *Ind. Eng. Chem., Process Des. Dev.* **10,** 108 (1971).
24. Kondis, E. F., and Dranoff, J. S., *AIChE Symp. Ser.* **67,** 25 (1971).
25. Kondis, E. F., and Dranoff, J. S., *Adv. Chem. Ser.* **102,** 171 (1971).
26. Ruthven, D. M., "Properties and Application of Zeolites," p. 43. The Chemical Society, London, 1980.